

Optimal modularity for nucleation in network-organized Ising model

Hanshuang Chen and Zhonghuai Hou*

*Hefei National Laboratory for Physical Sciences at Microscales & Department of Chemical Physics,
University of Science and Technology of China, Hefei, 230026, China*

(Dated: August 22, 2018)

We study nucleation dynamics of Ising model in a topology that consists of two coupled random networks, thereby mimicking the modular structure observed in real-world networks. By introducing a variant of a recently developed forward flux sampling method, we efficiently calculate the rate and elucidate the pathway for nucleation process. It is found that as the network modularity becomes worse the nucleation undergoes a transition from two-step to one-step process. Interestingly, the nucleation rate shows a nonmonotonic dependency on the modularity, in which a maximal nucleation rate occurs at a moderate level of modularity. A simple mean field analysis is proposed to qualitatively illustrate the simulation results.

PACS numbers: 89.75.Hc, 64.60.Q-, 05.50.+q

I. INTRODUCTION

In the last decade, critical phenomena in complex networks have received an enormous amount of attention in the field of statistical physics and many other disciplines (see, for example, a recent review [1]). Extensive research interests have focused on the onset of critical behaviors in diverse network topology, which included a wide range of issues: percolation phenomenon [2–5], epidemic thresholds [6, 7], order-disorder transitions [8–12], synchronization [13, 14], self-organized criticality [15, 16], nonequilibrium pattern formation [17], etc. However, there is much less attention paid to the dynamics/kinetics of phase transition itself in complex network, such as nucleation in a first-order phase transition.

Nucleation is a fluctuation-driven process that initiates the decay of a metastable state into a more stable one [18]. A first-order phase transition usually involves the nucleation and growth of a new phase. Many important phenomena in nature, including crystallization [19], glass formation [20], and protein folding [21], etc., are associated with nucleation. Despite its apparent importance, many aspects of nucleation process are still unclear and deserve more investigations. The Ising model, which is a paradigm for many phenomena in statistical physics, has been widely used to study the nucleation process. Despite its simplicity, Ising model has made important contributions to the understanding of nucleation phenomena in equilibrium systems and is likely to yield important insights also for nonequilibrium systems. In two-dimensional lattices, for instance, shear can enhance the nucleation rate and the rate peaks at an intermediate shear rate [22], a single impurity may considerably enhance the nucleation rate [23], and the existence of a pore may lead to two-stage nucleation and the overall nucleation rate can reach a maximum level at an intermediate pore size [24]. Nucleation pathway of Ising model

in three-dimensional lattice has also been studied using transition path sampling approach [25]. In addition, Ising model has been frequently used to test the validity of classical nucleation theory (CNT) [26–30]. However, all these studies are limited to regular lattices in Euclidean space. Since many real systems can be properly modeled by network-organized structure, it is thus natural to ask how the topology of a networked system affects the nucleation process of Ising model.

In a recent work [31], we have studied nucleation dynamics on scale-free networks, in which we found that nucleation starts from, on average, nodes with more lower degrees, and the rate for nucleation decreases exponentially with network size and the size of critical nucleus increase linearly with network size, implying that nucleation is relevant only for a finite-size network. Herein, we want to study nucleation dynamics of Ising model in a modular network composed of two coupled random networks. It is known that many real-world networks, as diverse as from social networks to biological networks, have found to exhibit modularity structures [32, 33], that is, links within modules are much more denser than those between modules. Many previous studies have revealed that such modular structures have a significant impact on the dynamics taking place on the networks, such as synchronization [34, 35], neural excitability [36], spreading dynamics [37, 38], opinion formation [39, 40], and Ising phase transition [41–43]. In particular, for majority model [39] and Ising model [41–43] in modular networks, it has been shown that there exists a region in a discontinuous transition where modular order phase and global order phase coexist. However, these studies mainly focused on phase diagrams in parameters space, and did not make detailed investigation for the transition process from a phase to another that may undergo a nucleation process.

Since nucleation is an activated process that occurs extremely slow, brute-force simulation is prohibitively expensive. To overcome this difficulty, we will use a variant of a recently developed simulation method, forward flux sampling (FFS) [44]. This method allows us to calculate

*Electronic address: hzhlj@ustc.edu.cn

nucleation rate and determine the properties of ensemble toward nucleation pathways. We found that as the degree of network modularity decreases nucleation goes through a transition from two-step to one-step process, and the rate exhibits a maximum at an intermediate degree of modularity. Free energy profiles for different modularity obtained by umbrella sampling (US) [45] and a simple mean-field (MF) analysis help us understand the FFS results.

This paper is organized as follows. In Sec.II, we describe the details of our model and the simulation method applied to this system. In Sec.III, we present the results for the nucleation rate and pathway in modular networks. In Sec.IV, a simple mean field analysis is used to qualitatively illustrate the simulation results. At last, discussion and main conclusions are addressed in Sec.V.

II. MODEL AND SIMULATION DETAILS

Consider a network consisting of N nodes arranged into two modules with N_1 and N_2 nodes. For simplicity, we only consider the case of $N_1 = N_2 = N/2$ throughout this paper. The connection probability between a pair of nodes belonging to the same module is ρ_i , while that for nodes belonging to different modules is ρ_o . The parameter $\sigma = \frac{\rho_o}{\rho_i} \in [0, 1]$, defined as the ratio of inter- to intra-modular connectivity, measures the degree of modularity. The higher degree of modularity of a network is, the smaller value of σ is. As $\sigma \rightarrow 0$, the network becomes two isolated clusters, while as $\sigma \rightarrow 1$, the network approaches a Erdős-Rényi (ER) random network. When σ is varied the total number of links of the network is kept unchanged, $\frac{N\langle k \rangle}{2}$, where $\langle k \rangle$ is the average degree. This restriction leads to $\rho_i = \frac{2\langle k \rangle}{N(1+\sigma)}$ and $\rho_o = \frac{2\langle k \rangle\sigma}{N(1+\sigma)}$. Each node is endowed with an Ising spin variable s_i that can be either +1 (up) or -1 (down). The Hamiltonian of the system is given by

$$H = -J \sum_{i < j} a_{ij} s_i s_j - h \sum_i s_i, \quad (1)$$

where $J (> 0)$ is the coupling constant and h is the external magnetic field. The elements of the adjacency matrix of the network take $a_{ij} = 1$ if nodes i and j are connected and $a_{ij} = 0$ otherwise.

Our simulation is performed by Metropolis spin-flip dynamics [46], in which we attempt to flip each spin once, on average, during each Monte Carlo (MC) cycle. In each attempt, a randomly chosen spin is flipped with the probability $\min(1, e^{-\beta\Delta E})$, where $\beta = 1/(k_B T)$ and k_B is the Boltzmann constant and T is the temperature, and ΔE is the energy difference due to the flipping process. Here, we set $J = 1$, $h > 0$, $T < T_c$ (T_c is the critical temperature), and start with a metastable state in which $s_i = -1$ for most of the spins. The system will stay in that state for a significantly long time before undergoing a nucleation transition to a more stable state with most

spins pointing up. We are interested in the pathway and rate for this nucleation process.

FFS method has been used to calculate rate constants and transition paths for rare events in equilibrium and nonequilibrium systems [22–24, 44, 47, 48]. This method uses a series of interfaces in phase space between the initial and final states to force the system from the initial state A to the final state B in a ratchet-like manner. Before the simulation begin, an order parameter λ is first defined, such that the system is in state A if $\lambda < \lambda_0$ and it is in state B if $\lambda > \lambda_M$. A series of nonintersecting interfaces λ_i ($0 < i < M$) lie between states A and B , such that any path from A to B must cross each interface without reaching λ_{i+1} before λ_i . The algorithm first runs a long-time simulation which gives an estimate of the flux $\bar{\Phi}_{A,0}$ escaping from the basin of A and generates a collection of configurations corresponding to crossings of interface λ_0 . The next step is to choose a configuration from this collection at random and use it to initiate a trial run which is continued until it either reaches λ_1 or returns to λ_0 . If λ_1 is reached, store the configuration of the end point of the trial run. Repeat this step, each time choosing a random starting configuration from the collection at λ_0 . The fraction of successful trial runs gives an estimate of the probability of reaching λ_1 without going back into A , $P(\lambda_1|\lambda_0)$. This process is repeated, step by step, until λ_M is reached, giving the probabilities $P(\lambda_{i+1}|\lambda_i)$ ($i = 1, \dots, M-1$). Finally, we get the transition rate R from A to B , which is the product of the flux $\bar{\Phi}_{A,0}$ and the probability $P(\lambda_M|\lambda_0) = \prod_{i=0}^{M-1} P(\lambda_{i+1}|\lambda_i)$ of reaching λ_M from λ_0 without going into A . The detailed descriptions of FFS method see Ref.[49].

However, conventional FFS method will become very inefficient if one intermediate metastable state exists between initial state and final state, as a two-step nucleation process demonstrated in Fig.1. This is because that sampling paths will be trapped in these long-lived metastable states so that they hardly return to initial state. To solve this problem, we will perform instead two-step samplings from initial down-spin state to intermediate metastable state, and then to final up-spin state, giving the two-step rates, R_1 and R_2 , respectively. Since the total mean time for nucleation is simply the sum of the mean time of the two-step process, the total rate can be expressed as $R = (R_1^{-1} + R_2^{-1})^{-1}$. To determine the location of the intermediate state, during FFS we monitor the sampling time for the probability $P(\lambda_{i+1}|\lambda_i)$ between two neighboring interfaces. If the sampling time spent on between interfaces i and $i+1$ is much more than its previous step and the probability $P(\lambda_{i+1}|\lambda_i)$ is nearly one, we consider the i th interface as the location of the intermediate state. If such conditions do not meet during the whole sampling, the intermediate metastable state does not exist, meaning that nucleation is a one-step process. Note that the method is straightforward to generalize to a multi-step nucleation process.

Here, we define the order parameter λ as the total number of up spins in the networks. The spacing between in-

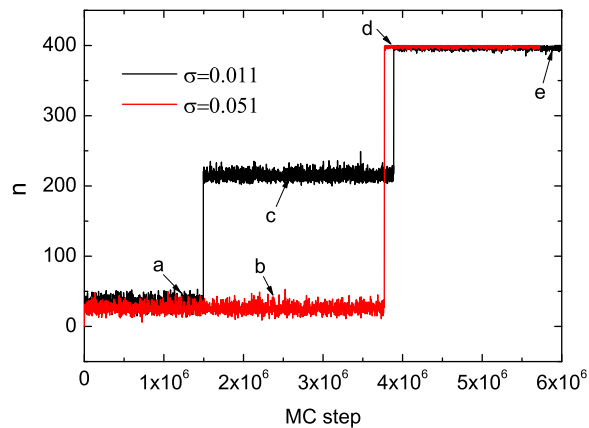


FIG. 1: (Color online) Typical time evolutions of the number of up spins λ . It is shown that the system undergoes a two-step nucleation process for $\sigma = 0.011$ and a one-step nucleation process for $\sigma = 0.051$. The representative network configurations at different moments indicated by arrows are shown in Fig.2. Other parameters are $N = 400$, $\langle k \rangle = 6$, $T = 2.0$, and $h = 1.2$.

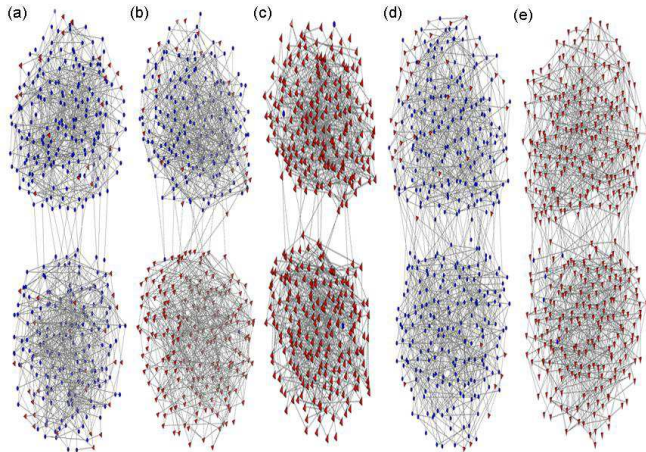


FIG. 2: (Color online) Five representative network configurations at different moments indicated in Fig.1, where down-spin nodes and up-spin nodes are denoted by blue circles and red triangles, respectively. (a)-(c) correspond to the case of $\sigma = 0.011$ and (d)-(e) correspond to the case of $\sigma = 0.051$.

interfaces is fixed at 3 up spins, but the computed results do not depend on this spacing. We perform 1000 trials per interface for each FFS sampling, from which at least 100 configurations are saved at each interface in order to investigate the statistical properties of an ensemble of reactive pathways to nucleation. The results are obtained by averaging over 10 independent FFS samplings and 50 different network realizations.

III. RESULTS

To begin with, in Fig.1 we exhibit typical time evolutions of the number of up spins λ corresponding to two different values of network modularity $\sigma = 0.011$ and $\sigma = 0.051$ via brute-force simulations, with relevant parameters $N = 400$, $\langle k \rangle = 6$, $T = 2.0$, and $h = 1.2$. It is clearly observed that the system undergoes a two-step nucleation process for $\sigma = 0.011$ and a one-step nucleation process for $\sigma = 0.051$. We also plot several representative configurations in Fig.2, corresponding to different phases of the system, respectively. Before the nucleation happening, the system lies in a metastable state, where most of the nodes are in down-spin state (indicated by blue circles), as shown in Fig.2(a) and Fig.2(d). When the network modularity is very good, the system enters into an intermediate metastable state via the first-step nucleation, where nodes in one of modules are in up-spin state (indicated by red triangles), while nodes in the other module are still in down-spin state, as shown in Fig.2(b). When the network modularity becomes worse, such an intermediate metastable state disappears so that the nucleation becomes a one-step process. Finally, the system will enter into the most stable state, where almost all spins are in up-spin state, as shown in Fig.2(c) and Fig.2(e). Moreover, we note that that the nucleation process typically takes the order of 10^6 or more MC steps that is computationally costly. Therefore, in what follows we will give the results obtained by FFS method.

The nucleation rate R as a function of σ is plotted in Fig.3(a), with relevant parameters being the same as those in Fig.1 except for $h = 1.0$. One can see that as σ increases R reaches a maximum R_c at $\sigma \simeq 0.031$ and then decreases. Obviously, there exists a maximal nucleation rate that occurs at a moderate degree of network modularity. In Fig.3(b), we plot the results of the nucleation rates, R_1 and R_2 , for two-steps process as functions of σ . As σ increases, R_1 seems to exponentially decreases with σ , while R_2 increases monotonically until $\sigma = 0.051$ is reached. For $\sigma > 0.051$, nucleation becomes one-step process so that R_2 can not be well defined and the overall nucleation rate is only determined by R_1 . From Fig.3(b) one can find that R_2 is much lower than R_1 when the value of σ is relatively small, so that R is dominantly determined by the second step nucleation. While for $\sigma > 0.031$, R is almost determined only by the first step nucleation. Thus, there exists a region $0.001 < \sigma < 0.031$ where R is determined by both R_1 and R_2 . Note that we have also made extensive simulations for other parameters such as $h = 0.7, 1.2$ and $T = 1.5, 1.8$, and found that the qualitative features of the above results do not change (results now shown).

To further understand the above results, we calculate free energy of the system by US method, in which we have used a bias potential $0.1k_B T(\lambda - \bar{\lambda})^2$, with $\bar{\lambda}$ being the center of each window. The free energy ΔF as a function of λ for three different values of σ are depicted in Fig.4(a). For $\sigma = 0.001$ and $\sigma = 0.031$, there are two free-energy

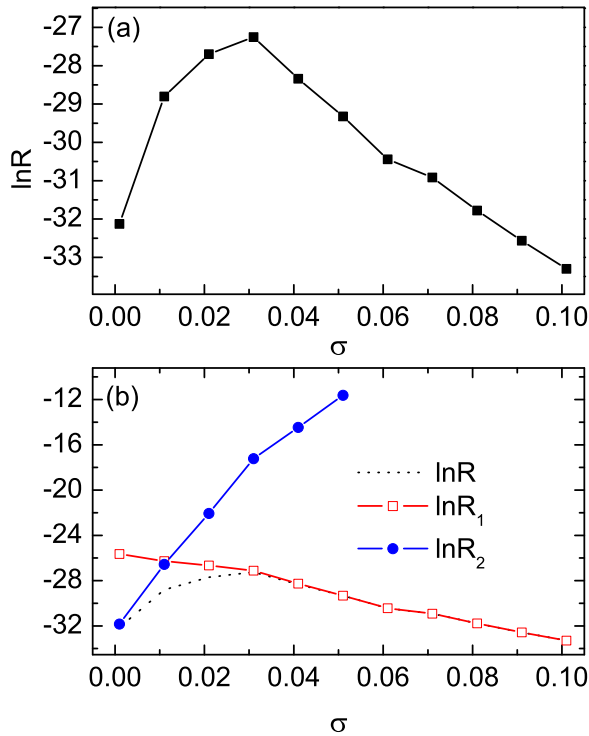


FIG. 3: (Color online) (a) The logarithm of nucleation rate $\ln R$ as a function of the degree of modularity σ . (b) $\ln R_1$ (squares) and $\ln R_2$ (circles) as a function of σ , and dotted line indicates the overall rate $\ln R$. The parameters are same as in Fig.1 except for $h = 1.0$.

maximums, occurring at the locations of critical nucleus of $\lambda = \lambda_1^*$ and $\lambda = \lambda_2^*$, respectively. This picture is consistent with the two-step nucleation process described before. For a larger $\sigma = 0.101$, just the first free-energy barrier is present, implying that the nucleation becomes one-step process. With the increment of σ , λ_1^* moves to a larger value while the value of λ_2^* gets smaller, as shown in Fig.4(b). Fig.4(c) shows that the first free-energy barrier ΔF_1^* , defined as the difference between the free energy at λ_1^* and the first minimum in free energy ($\lambda = 23$), nearly increases linearly with σ , while the second free-energy barrier ΔF_2^* (definition is similar to that of ΔF_1^* , and the second minimum in free energy is an increasing function of σ , within the range $\lambda \in [78, 93]$) decreases monotonically with σ until ΔF_2^* vanishes at $\sigma > 0.051$, which is in agreement with the result of Fig.3(b).

IV. MEAN FIELD ANALYSIS

In order to unveil possible mechanism behind the above phenomenon, we will present an analytical understanding by CNT and simple MF approximation. Firstly, let us assume, for the first-step nucleation, that λ nodes are in up-spins and the remaining nodes are in down-spins in one of modules (say module I for convenience),

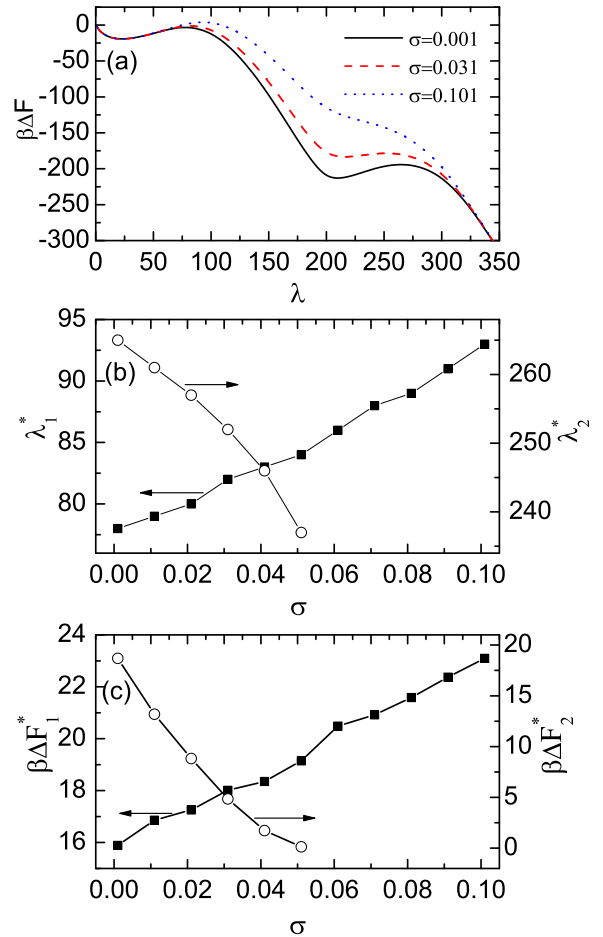


FIG. 4: (Color online) (a) Free energy ΔF as a function of λ for three different $\sigma = 0.001, 0.031, 0.101$. For smaller σ two free-energy barriers are clearly observed, while for larger σ the second one vanishes. (b) The size of critical nucleus λ_1^* and λ_2^* , and (c) the free-energy barriers ΔF_1^* and ΔF_2^* , as functions of σ . The other parameters are the same as Fig.2.

and all the nodes in the other module (module II) are in down-spins. The energy change due to the spin-flip of these λ nodes can be expressed as the sum of two parts $\Delta U_1 = -2h\lambda + 2JN_1^{in}$, where the first part denotes the energy loss due to the creation of λ up-spins, which favors the growth of the nucleus, while the second part denotes the energy gain due to the formation of N_1^{in} new interfacial links between up and down spins, which disfavors the growth of the nucleus. According to MF approximation, N_1^{in} can be written as $N_1^{in} = \rho_i \lambda (\frac{N}{2} - \lambda) + \rho_o \lambda \frac{N}{2}$, where the first part and the second part arise from interfacial links inside module I and between modules, respectively. For the second-step nucleation, we assume that all the nodes in module I are in up-spins, and λ nodes are in up-spins and the remaining nodes are in down-spins in module II. This process creates new interfacial links inside module II, and at the same time removes old interfacial links between module I and module II. Thus, the energy change for this process is

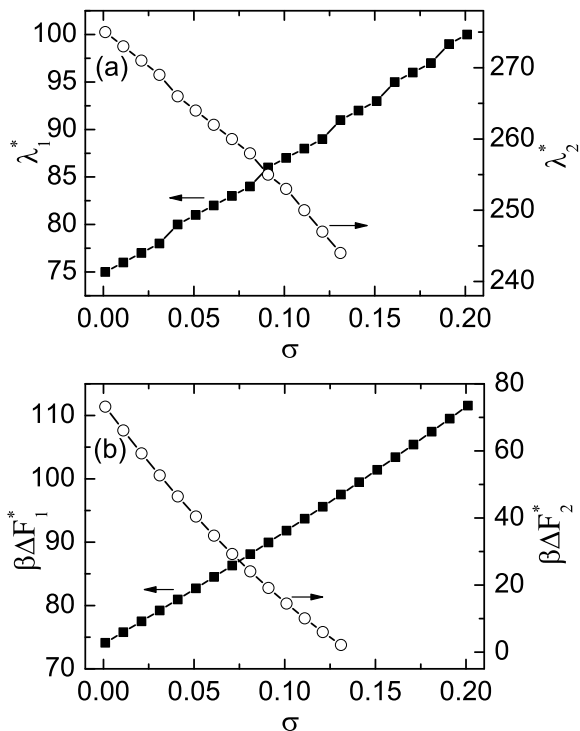


FIG. 5: The results of mean field analysis. (a) The size of critical nucleus λ_1^* and λ_2^* , and (b) the free-energy barriers ΔF_1^* and ΔF_2^* , as functions of σ . The other parameters are the same as Fig.2.

$\Delta U_2 = -2h\lambda + 2JN_2^{in}$ where $N_2^{in} = \rho_i\lambda\left(\frac{N}{2} - \lambda\right) - \rho_o\lambda\frac{N}{2}$ is the net number of the interfacial links. The entropy changes for the two nucleation processes are both $\Delta S = -\frac{k_B N}{2} \left[\frac{2\lambda}{N} \ln\left(\frac{2\lambda}{N}\right) + \left(1 - \frac{2\lambda}{N}\right) \ln\left(1 - \frac{2\lambda}{N}\right) \right]$. Then, the changes of free energy for the two-step processes are $\Delta F_i = \Delta U_i - T\Delta S$ ($i = 1, 2$). In Fig.5 we give the analytical results of the critical nucleus and free-energy barriers as functions of the network modularity. Clearly, the analysis qualitatively agrees with the simulation results

of Fig.4. From Fig.5, one can see that with the increment of σ the size of the first critical nucleus and the height of the first free-energy barrier increase almost linearly, while the size of the second critical nucleus and the height of the second free-energy barrier decrease until $\sigma \simeq 0.13$ is reached. This implies that the analysis also predicts the extinction of the second nucleation stage, but this prediction obviously overestimates the transition value of σ .

V. CONCLUSIONS

In conclusion, we have studied nucleation dynamics of Ising model in modular networks consisted of two random networks. Using FFS method, we found that as the network modularity gradually becomes worse a transition occurs from one-step to two-step nucleation process. Interestingly, the nucleation rate is a nonmonotonic function of the degree of modularity and a maximal rate exists for an intermediate level of modularity. Using US method, we obtained free energy profiles at different network modularity, from which one can see that two free-energy barriers exist for very good modularity and the second one vanishes when the network modularity becomes worse. This picture further confirms the FFS results. Finally, a mean field analysis is employed to understand the nature of nucleation in modular networks and the simulation results. Since stochastic fluctuation and the coexistent of multi-states are ubiquitous in social and biological systems, our study may shed valuable insights into fluctuation-driven transition phenomena taking place in network-organized systems with modular structures.

Acknowledgments

This work was supported by NSFC (Nos. 20933006, 20873130).

-
- [1] S. N. Dorogovtsev, A. V. Goltsev, and J. F. F. Mendes, *Rev. Mod. Phys.* **80**, 1275 (2008).
 - [2] R. Cohen, K. Erez, D. ben Avraham, and S. Havlin, *Phys. Rev. Lett.* **85**, 4626 (2000).
 - [3] D. S. Callaway, M. E. J. Newman, S. H. Strogatz, and D. J. Watts, *Phys. Rev. Lett.* **85**, 5468 (2000).
 - [4] M. E. J. Newman, *Phys. Rev. Lett.* **89**, 208701 (2002).
 - [5] R. Cohen, D. ben Avraham, and S. Havlin, *Phys. Rev. E* **66**, 036113 (2002).
 - [6] R. Pastor-Satorras and A. Vespignani, *Phys. Rev. Lett.* **86**, 3200 (2001).
 - [7] C. Castellano and R. Pastor-Satorras, *Phys. Rev. Lett.* **105**, 218701 (2010).
 - [8] A. Aleksiejuk, J. A. Holysta, and D. Stauffer, *Physica A* **310**, 260 (2002).
 - [9] G. Bianconi, *Phys. Lett. A* **303**, 166 (2002).
 - [10] S. N. Dorogovtsev, A. V. Goltsev, and J. F. F. Mendes, *Phys. Rev. E* **66**, 016104 (2002).
 - [11] M. Leone, A. Vázquez, A. Vespignani, and R. Zecchina, *Eur. Phys. J. B* **28**, 191 (2002).
 - [12] C. P. Herrero, *Phys. Rev. E* **69**, 067109 (2004).
 - [13] T. Nishikawa, A. E. Motter, Y.-C. Lai, and F. C. Hoppensteadt, *Phys. Rev. Lett.* **91**, 014101 (2003).
 - [14] J. Gómez-Gardeñes, Y. Moreno, and A. Arenas, *Phys. Rev. Lett.* **98**, 034101 (2007).
 - [15] K.-I. Goh, D.-S. Lee, B. Kahng, and D. Kim, *Phys. Rev. Lett.* **91**, 148701 (2003).
 - [16] A. E. Motter and Y. C. Lai, *Phys. Rev. E* **66**, 065102 (2002).
 - [17] H. Nakao and A. S. Mikhailov, *Nat. Phys.* **6**, 544 (2010).
 - [18] D. Kashchiev, *Nucleation: basic theory with applications* (Butterworths-Heinemann, Oxford, 2000).

- [19] L. Gránásy and F. Iglói, *J. Chem. Phys.* **107**, 3634 (1997).
- [20] G. Johnson, A. I. Melćuk, H. Gould, W. Klein, and R. D. Mountain, *Phys. Rev. E* **57**, 5707 (1998).
- [21] A. R. Fersht, *Proc. Natl. Acad. Sci. USA* **92**, 10869 (1995).
- [22] R. J. Allen, C. Valeriani, S. Tanase-Nicola, P. R. ten Wolde, and D. Frenke, *J. Chem. Phys.* **129**, 134704 (2008).
- [23] R. P. Sear, *J. Phys. Chem. B* **110**, 4985 (2006).
- [24] A. J. Page and R. P. Sear, *Phys. Rev. Lett.* **97**, 065701 (2006).
- [25] A. C. Pan and D. Chandler, *J. Phys. Chem. B* **108**, 19681 (2004).
- [26] M. Acharyya and D. Stauffer, *Eur. Phys. J. B* **5**, 571 (1998).
- [27] V. A. Shneidman, K. A. Jackson, and K. M. Beatty, *J. Chem. Phys.* **111**, 6932 (1999).
- [28] S. Wonzak, R. Strey, and D. Stauffer, *J. Chem. Phys.* **113**, 1976 (2000).
- [29] K. Brendel, G. T. Barkema, and H. van Beijeren, *Phys. Rev. E* **71**, 031601 (2005).
- [30] S. Ryu and W. Cai, *Phys. Rev. E* **81**, 030601(R) (2010).
- [31] H. Chen, C. Shen, Z. Hou, and H. Xin, arXiv:1008.0704 (2010).
- [32] M. E. J. Newman, *Proc. Natl. Acad. Sci. USA* **103**, 8577 (2006).
- [33] S. Fortunato, *Phys. Rep.* **486**, 75 (2010).
- [34] A. Arenas, A. Díaz-Guilera, and C. J. Pérez-Vicente, *Phys. Rev. Lett.* **96**, 114102 (2006).
- [35] D. Li, I. Leyva, J. A. Almendral, I. Sendiña Nadal, J. M. Buldú, S. Havlin, and S. Boccaletti, *Phys. Rev. Lett.* **101**, 168701 (2008).
- [36] C. Zhou, L. Zemanová, G. Zamora, C. C. Hilgetag, and J. Kurths, *Phys. Rev. Lett.* **97**, 238103 (2006).
- [37] Z. Liu and B. Hu, *Europhys. Lett.* **72**, 315 (2005).
- [38] L. Huang, K. Park, and Y.-C. Lai, *Phys. Rev. E* **73**, 035103 (2006).
- [39] R. Lambiotte and M. Ausloos, *J. Stat. Mech.* p. P08026 (2007).
- [40] R. Lambiotte, M. Ausloos, and J. A. Holyst, *Phys. Rev. E* **75**, 030101 (2007).
- [41] R. K. Pan and S. Sinha, *Europhys. Lett.* **85**, 68006 (2009).
- [42] S. Dasgupta, R. K. Pan, and S. Sinha, *Phys. Rev. E* **80**, 025101(R) (2009).
- [43] K. Suchecki and J. A. Holyst, *Phys. Rev. E* **80**, 031110 (2009).
- [44] R. J. Allen, P. B. Warren, and P. R. ten Wolde, *Phys. Rev. Lett.* **94**, 018104 (2005).
- [45] J. S. van Duijneveldt and D. Frenkel, *J. Chem. Phys.* **96**, 15 (1992).
- [46] D. P. Landau and K. Binder, *A Guide to Monte Carlo Simulations in Statistical Physics* (Cambridge University Press, Cambridge, 2000).
- [47] C. Valeriani, R. J. Allen, M. J. Morelli, D. Frenkel, and P. R. ten Wolde, *J. Chem. Phys.* **127**, 114109 (2007).
- [48] R. J. Allen, D. Frenkel, and P. R. ten Wolde, *J. Chem. Phys.* **124**, 024102 (2006).
- [49] R. J. Allen, C. Valeriani, and P. R. ten Wolde, *J. Phys.: Condens. Matter* **21**, 463102 (2009).